Published August 5, 2002

JCB Article

MAP2 is required for dendrite elongation, PKA anchoring in dendrites, and proper PKA signal transduction

Akihiro Harada, Junlin Teng, Yosuke Takei, Keiko Oguchi, and Nobutaka Hirokawa

Department of Cell Biology and Anatomy, Graduate School of Medicine, University of Tokyo, Hongo 7-3-1, Bunkyo-ku, Tokyo, 113-0033, Japan

Microtubule-associated protein 2 (MAP2) is a major component of cross-bridges between microtubules in dendrites, and is known to stabilize microtubules. MAP2 also has a binding domain for the regulatory subunit II of cAMP-dependent protein kinase (PKA). We found that there is reduction in microtubule density in dendrites and a reduction of dendritic length in MAP2-deficient mice. Moreover, there is a significant reduction of various subunits of PKA in dendrites and total amounts of various PKA subunits in hippocampal tissue and cultured neurons. In MAP2-deficient cultured neurons, the induction rate of phosphorylated CREB after forskolin stimulation was much lower than in wild-type neurons. Therefore, MAP2 is an anchoring protein of PKA in dendrites, whose loss leads to reduced amount of dendritic and total PKA and reduced activation of CREB.

Introduction

Microtubule-associated protein (MAP)* 2, the most abundant MAP in the brain, mainly localizes to the somatodendritic compartments in neurons. MAP2 has three or four microtubule binding domains at the COOH-terminal, and is involved in microtubule assembly and stabilization in dendrites (Goedert et al., 1991; Matus, 1994). It is also a major component of cross-bridges between microtubules (MTs) or between MTs and other cytoskeletal components in dendrites as revealed by quick freeze deep etch microscopy and immunoelectron microscopy (Shiomura and Hirokawa, 1987; Hirokawa et al., 1988). Overexpression of MAP2 resulted in intracellular bundling of MTs and process formation of nonneuronal cells (Lewis et al., 1989; Chen et al., 1992; Takemura et al., 1992; Hirokawa, 1994). Inhibition of MAP2 production by the addition of MAP2 antisense oligonucleotides into the culture medium of cerebellar macroneurons (Caceres et al., 1992) or the expression of antisense construct in the embryonic carcinoma cell lines resulted in the inhibition of the initial neurite formation and outgrowth (Dinsmore and Solomon, 1991). These results indicated MAP2 is essential for dendritic growth by selectively stabilizing dendritic MTs.

MAP2 is also known to have a domain that binds to the regulatory subunit II of cAMP-dependent protein kinase (PKA) near its NH_2 terminus (Vallee et al., 1981; Theurkauf and Vallee, 1982). The catalytic subunit of PKA binds to the regulatory subunit I (RI) or II (RII) in an inactive state, and the inactive complex exists as a heterotetramer (two catalytic and two regulatory subunits). The catalytic subunits dissociate from RI or RII when intracellular cAMP binds to the cAMP binding sites of RI or RII. In neurons, RII is the major regulatory subunit and comprises 85–90% of total regulatory subunit of PKA (Stein et al., 1987; Ventra et al., 1996). Thus, the localization of RII determines the localization of PKA itself in neurons, whose kinase activity is known to be involved in various biological functions in neurons, including the formation of long-term memory in mice (Abel et al., 1997; Malleret et al., 2001). As MAP2 is highly enriched in the dendritic cytoskeleton, it has been assumed that it is one of the major PKA-anchoring proteins in dendrites, and thus assumed to play roles in PKA signal transduction. However, the role of MAP2 in PKA signal transduction has not been intensively examined in spite of its abundance in neurons. Therefore, to know the role of MAP2 in the intracellular structure and the signal transduction by PKA in neurons, we disrupted the *map2* gene by homologous recombination in embryonic stem cells and made MAP2-

Address correspondence to N. Hirokawa, Department of Cell Biology and Anatomy, Graduate School of Medicine, University of Tokyo, Hongo 7-3-1, Bunkyo-ku, Tokyo 113-0033, Japan. Tel: 81-3-5841-3326. Fax: 81-3-5802-8646. E-mail: hirokawa@m.u-tokyo.ac.jp

*Abbreviations used in this paper: CREB, cAMP-responsive element binding protein; MAP, microtubule-associated protein; MT, microtubule; PKA, cAMP-dependent protein kinase; RI/RII, regulatory subunit I/II.

Key words: knockout; microtubule; cAMP-dependent protein kinase; regulatory subunit; CREB

Published August 5, 2002

deficient mice. In our previous paper (Teng et al., 2001), we analyzed MAP2 MAP1B double knockout mice and showed that the double knockout mice had decreased microtubule spacing in dendrites, decreased dendritic elongation of immature hippocampal neurons, fiber tract malformations, and defects in neuronal migration. These results indicated that MAP2 and MAP1B act synergistically in neuronal migration and dendritic extension. However, the unique role of MAP2 on MT organization and PKA signal transduction was not reported in the previous paper. In this paper, we report that MAP2 itself is important as a structural protein and as an anchoring protein of PKA in dendrites whose loss leads to reduced dendritic and total PKA and reduced activation of cAMP-responsive element binding protein (CREB).

Results

Targeting the *map2* gene

To disrupt the endogenous *map2* gene, a targeting vector was constructed (Harada et al., 1998) with the *neo* gene inserted into the fifteenth exon (Kalcheva et al., 1995) that encodes the first MT binding domain and the preceding proline-rich domain (Teng et al., 2001). Homozygous mutant (*map2* $^{-/-}$) animals were fertile and have shown no evidence of premature mortality, but they were smaller and 10–20% less in body weight than their littermate controls. However, their brain weight was not significantly less than their littermate controls.

Microtubule density is reduced and fine structures are altered in dendrites of MAP2-deficient mice

To further investigate the morphological changes in *map2* $^{-/-}$ brains, we examined cerebellar tissue by electron microscopy. The gross cytoarchitecture and cell morphology of *map2* $^{-/-}$ cerebellum were indistinguishable from those of the control cerebellum. Our previous paper (Teng et al., 2001) reported decreased spacing between MTs in neurites of MAP2 MAP1B double knockout, but it did not report quantitation of the MT density of *map2* $^{-/-}$ dendrites. When we examined Purkinje cell dendrites, MT density in *map2* $^{-/-}$ mice (35.6 $\pm$ 8.5 MTs/μm^2 [mean $\pm$ SD]; n = 31) is 23% less than that in wild-type mice (46.3 $\pm$ 8.6; n = 25) ($P < 0.001$, Student's t test). Therefore, though MAP2 and MAP1B act synergistically in MT organization in dendrites as reported previously, the polymerization of dendritic MTs is affected by the absence of MAP2 alone.

Also in our previous paper (Teng et al., 2001), we were not able to detect changes in MT organization in *map2* $^{-/-}$ dendrites using conventional electron microscopy. Therefore, to further assess the structural changes in the dendrites of *map2* $^{-/-}$ mice, cerebellar Purkinje cell dendrites of *map2* $^{-/-}$ and wild-type mice were examined by quick-freeze, deep-etch electron microscopy, which was more suitable to examine cytoskeletal organization (Harada et al., 1994). In wild-type dendrites, we observed thick filamentous cross-bridges between MTs (Fig. 1, arrows), confirming our previous studies (Hirokawa et al., 1988; Chen et al., 1992). In *map2* $^{-/-}$ dendrites, the cross-bridges between MTs (Fig. 1, arrows) were thinner (for wild type, 7.08 $\pm$ 0.36 nm, 45 cross-bridges from two animals; for knockout, 4.38 $\pm$ 0.63, 28 cross-bridges from two animals) ($P < 0.01$). Globular structures were observed on the surface of MTs in wild-type dendrites (Fig. 1, arrowheads), but these globular structures were rarely observed in mutant dendrites. These observations led us to conclude that MAP2 was required to form thick cross-bridges between MTs, and that MAP2 was required for MT organization in the dendrites.

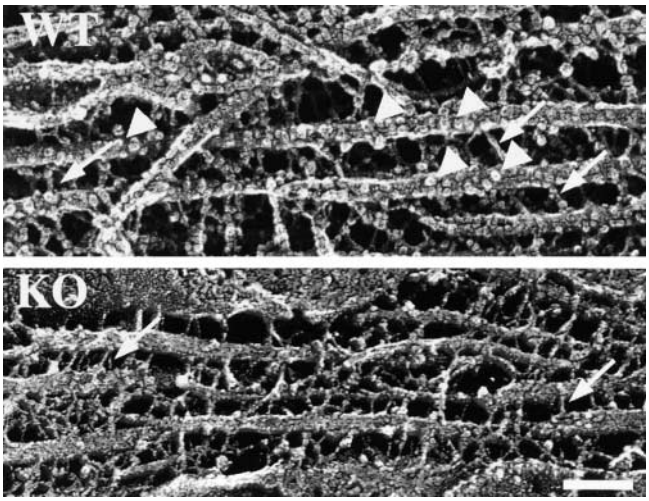

Figure 1. **The dendritic cytoskeleton of wild-type and MAP2 knockout mice.** Quick-frozen, deep-etched Purkinje cell dendrites of wild-type (WT) and *map2* $^{-/-}$ (KO) mice. Numerous cross-bridges (arrows) are observed between MTs. Cross-bridges in *map2* $^{-/-}$ dendrites (arrows) appears thinner than those in wild-type dendrites. On the surface of MTs, a number of globular structures (arrowheads) are observed in wild-type dendrites that are almost absent in *map2* $^{-/-}$ dendrites. Bar, 100 nm.

Dendrite length is reduced in MAP2-deficient neurons in vitro and in vivo

To examine the effect of MAP2 in neuronal maturation, we observed hippocampal neurons in culture. In our previous paper, we did not detect significant difference in the polarization process at days 0.5, 1, 1.5, 2, and 3 after plating between *map2* $^{-/-}$ and the control neurons (Teng et al., 2001). However, we did not report changes in *map2* $^{-/-}$ hippocampal culture at later stages. In our previous paper (Teng et al., 2001), the length of neurites of long-term cultured neurons could not be measured because we plated neurons so densely that we were unable to discriminate each neurite. Therefore, we plated the hippocampal neurons at a lower density and cultured for a long period (3 wk), the length of *map2* $^{-/-}$ dendrites was significantly (~30%) shorter than that of the control dendrites (Fig. 2, A and C): for WT1, 153 $\pm$ 54 μm n = 25 neurons; for WT2, 135 $\pm$ 50, n = 34; for WT3, 144 $\pm$ 58, n = 30; for KO1, 98 $\pm$ 34, n = 22; for KO2, 106 $\pm$ 35, n = 35; and for KO3, 92 $\pm$ 27, n = 33 ($P < 0.00001$, Post-hoc test). These results indicate that MAP2 is required for the dendrite extension at later stages in culture.

To assess the morphology of the dendritic trees in *map2* $^{-/-}$ hippocampal neurons in vivo, we stained hippocampal tissue by using the rapid Golgi method. When we observed the CA1 region of the hippocampus, apical dendrites of *map2* $^{-/-}$ hip-

Published August 5, 2002

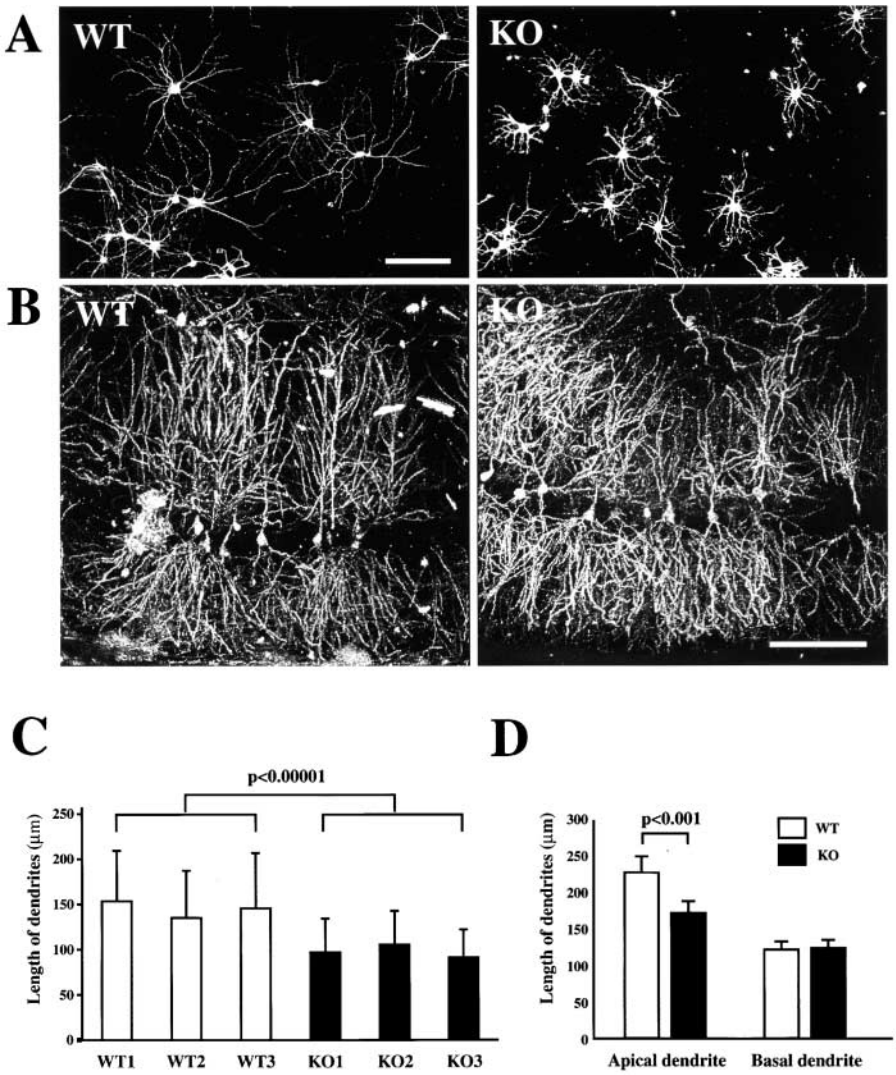

Figure 2. **Decreased length of dendrites in hippocampal neurons from *map2* $^{-/-}$ mouse.** (A) Hippocampal cells in culture for 3 wk stained with rhodamine phalloidin. Dendrites of *map2* $^{-/-}$ cells (KO) are shorter than wild-type cells (WT). Bar, 100 μm. (B) Pyramidal neurons in CA1 area of hippocampal tissues stained by the rapid Golgi method. Apical dendrites of *map2* $^{-/-}$ neurons (KO) are shorter than those of wild-type neurons (WT). However, the length of basal dendrites of *map2* $^{-/-}$ neurons is similar to that of wild-type neurons. Bar, 100 μm. (C) Quantitation of the average length of dendrites between wild-type (WT1–3) and *map2* $^{-/-}$ cells (KO1–3). The average lengths of *map2* $^{-/-}$ dendrites contained within a neuron are significantly shorter than those of wild-type dendrites (mean ± SD). $P < 0.00001$ (Post-hoc test). (D) Quantitation of the average length of apical and basal dendrites between wild-type (WT) and *map2* $^{-/-}$ cells (KO). The average lengths of *map2* $^{-/-}$ apical dendrites contained within a neuron are significantly shorter than those of wild-type dendrites (for *map2* $^{-/-}$ mice, 179 ± 15 μm; 11 dendrites from 11 tissue sections from two animals [we selected the longest dendrite from one section]; for wild-type mice, 229 ± 22; the number of samples and animals are the same as those of knockout) (mean ± SD). $P < 0.001$ (Post-hoc test).

pocampal neurons were shortened compared with wild-type dendrites, whereas the basal dendrites were not affected (Fig. 2 B). The length of mutant apical dendrites was 22% shorter than that of wild-type dendrites (Fig. 2 D), whereas the length of basal dendrites did not differ (for *map2* $^{-/-}$ mice, 120 ± 10 μm; 11 dendrites from 11 tissue sections [we selected the longest dendrite from one section] from two animals; for wild-type mice, 122 ± 11; the number of samples and animals are the same as those of knockout) (Fig. 2 D). Therefore, map2 is required for the morphology of the dendrites both in vivo and in vitro.

Various PKA subunits are reduced in *map2* $^{-/-}$ dendrites of hippocampal and cortical neurons

Next, we examined the localization of various PKA subunits in *map2* $^{-/-}$ and the control mice because MAP2 binds to the RII of PKA and binds to about one third of total PKA in brain (Vallee et al., 1981). Hippocampus and cerebral cortex from various ages of mice were examined because of their high content of PKA (Glantz et al., 1992; Ventra et al., 1996). In the control hippocampus, both the apical (Fig. 3, A and A′) and the basal dendrites of pyramidal neurons in the CA1 and CA3 regions exhibited high levels of PKA (RII α, β, and the catalytic subunits) The dendritic PKA staining is more apparent in early postnatal ages (2 wk of age; Fig. 3, A, A′, C, C′, E, E′, G, and G′), but is also observed in adult mice (8 wk of age; Fig. 4, A, B, and D). In addition to this dendritic staining, the mossy fiber axons (Fig. 3, mf) from the granule cells of dentate gyrus (Fig. 3, stained by anti-τ antibody in E″, F″, G″, and H″) contained RII β and the catalytic subunits (Fig. 3, A, A′, C, C′, G, and G′ and Fig. 4 A). RII α staining was very low in the mossy fiber axons (Fig. 3, E and E′). However, in *map2* $^{-/-}$ hippocampus, the dendritic staining of RII α, β, and the catalytic subunits reduced significantly (Fig. 3, B–B″, D–D″, F, F′, H, and H′ and Fig. 4, A′, B′, D′), whereas the axonal staining seemed relatively unaffected as revealed by the staining of mossy fiber in Fig. 3 (B and B′, mf). The axonal staining also seemed unaffected in the fimbria that includes axons from the hippocampal pyramidal neurons (unpublished data).

To confirm the reduction of various PKA subunits in *map2* $^{-/-}$ dendrites, we stained cerebral cortex. In the control cerebral cortex of adult mice, strong signals for PKA subunits were observed in neurons throughout the cortex, but it accumulated primarily in the apical dendrites and the

Published August 5, 2002

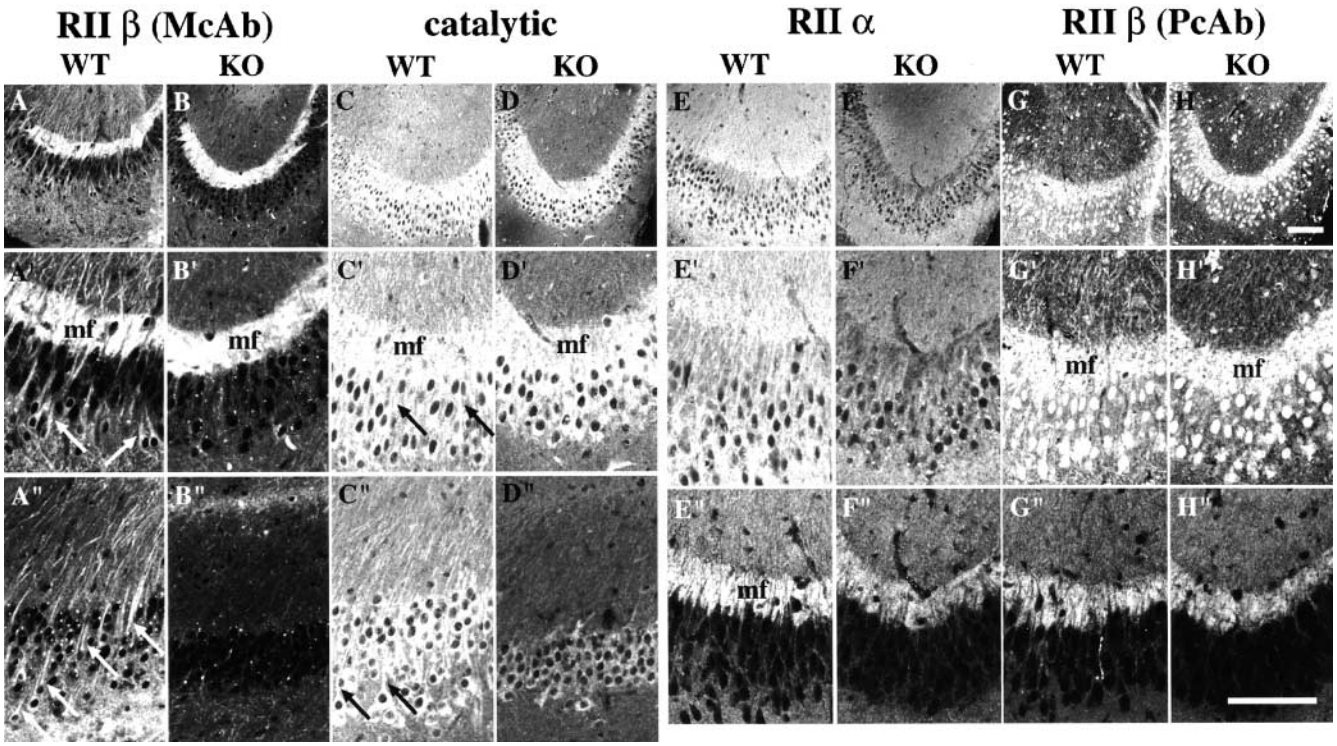

Figure 3. **Reduced expression of PKA in the dendrites of 2-wk-old wild-type and *map2* $^{-/-}$ hippocampus.** Low (A–H) and high (A′–H′) magnification view of CA3 region stained with anti–RII β monoclonal antibody (A, A′, B, and B′), anti–catalytic subunit antisera (C, C′, D, and D′), anti–RII α antisera (E, E′, F, and F′), and anti–RII β antisera (G, G′, H, and H′). High magnification view of CA1 region stained with anti–RII β monoclonal antibody (A′′ and B′′) and anti–catalytic subunit antisera (C′′ and D′′). E′′, F′′, G′′, and H′′ are the same sections as E′, F′, G′, and H′, respectively, stained with anti-τ antibody (tau-1) to show the localization of mossy fiber (mf). Arrows in A′, A′′, C′, and C′′ indicate the dendritic staining of PKA in wild-type pyramidal cells. Bars, 100 μm.

soma in the pyramidal neurons (Fig. 5, A–C). In *map2* $^{-/-}$ cortex, the signals in the soma were relatively unchanged, but those in the dendrites were significantly reduced (Fig. 5, A′–C′). Similar to the observation in the hippocampus, the content of RII β and the catalytic subunits seemed unchanged in the axonal compartments that were stained by tau-1 antibody (unpublished data).

To examine the content and the subcellular localization of various PKA subunits, we stained dissociated hippocampal cultured neurons. In hippocampal neurons, the staining of

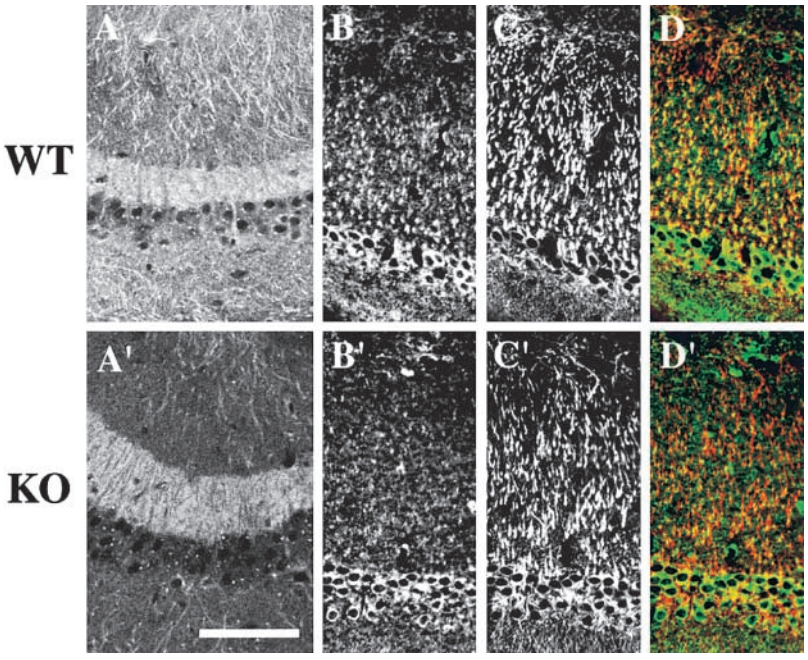

Figure 4. **Reduced expression of various subunits of PKA in the dendrites of adult wild-type and *map2* $^{-/-}$ hippocampus.** CA3 region (A and A′) and CA1 region (B–D and B′–D′) stained with anti–RII β monoclonal antibody (A and A′) and anti–catalytic subunit antisera (B and B′). The same sections stained with anti–catalytic subunit antisera (B and B′) were stained by anti-MAP1A monoclonal antibody (C and C′) to show the localization of dendrites and the merged figures between PKA catalytic subunit (green) and MAP1A (red) are shown in D and D′. Catalytic subunit is reduced in the dendrites of *map2* $^{-/-}$ hippocampal neurons. Bar, 100 μm.

Published August 5, 2002

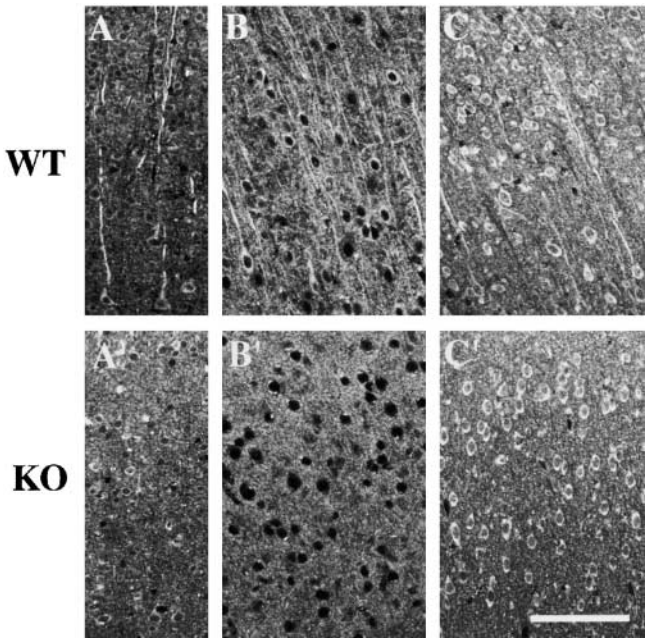

Figure 5. **Reduced expression of various subunits of PKA in the dendrites of adult wild-type and *map2* $^{-/-}$ cerebral cortex.** (A and A′) Sections stained with anti–RII α antisera. RII α staining is greatly reduced in the dendrites of *map2* $^{-/-}$ cortical neurons. Sections stained with anti–RII β monoclonal antibody (B and B′), and with anti–catalytic subunit antisera (C and C′). RII β and catalytic subunits are also reduced in the dendrites of *map2* $^{-/-}$ cortical neurons. Bar, 100 μm.

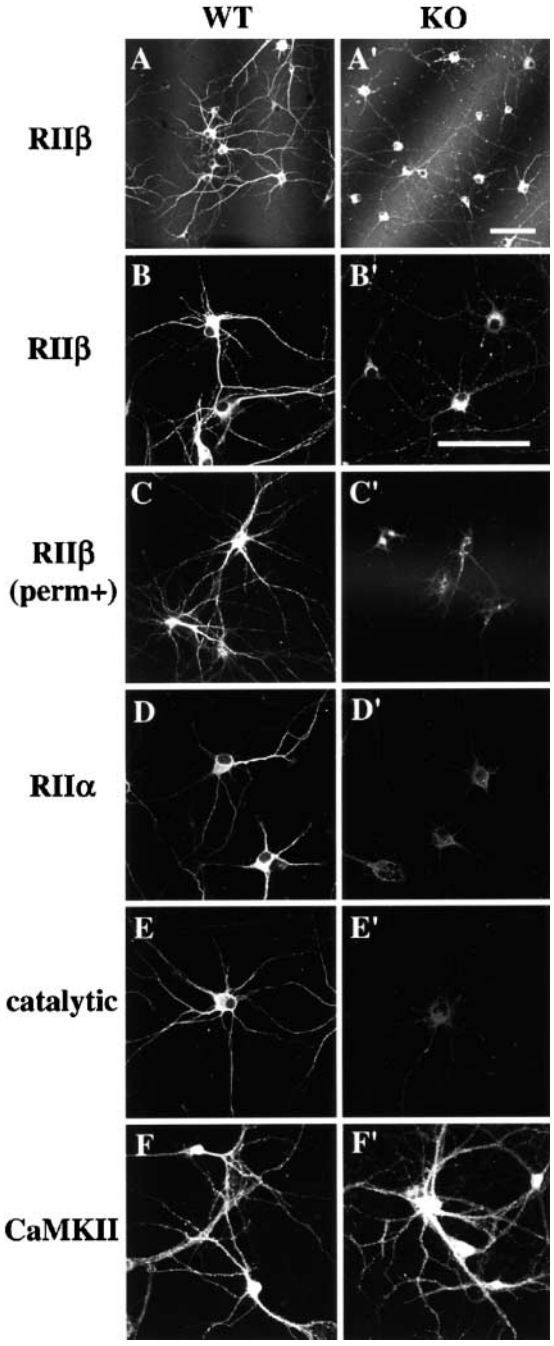

Figure 6. **Expression of various subunits of PKA in the hippocampal neurons of wild-type and *map2* $^{-/-}$ mice.** Hippocampal neurons were stained with anti–RII β monoclonal antibody (A–C and A′–C′), anti–RII α antisera (D and D′), anti–catalytic subunit antisera (E and E′), and anti–calcium/calmodulin-dependent kinase II β monoclonal antibody (F and F′). Neurons in C and C′ were permeabilized with 0.1% Triton X-100 before fixation. Bars, 50 μm.

PKA subunits (RIIα, β and the catalytic subunit) was weaker in the somatodendritic compartments of *map2* $^{-/-}$ neurons (Fig. 6, A′–E′) than wild-type neurons (Fig. 6, A–E), whereas the staining of Ca/calmodulin-dependent kinase in *map2* $^{-/-}$ neurons (Fig. 6 F′) was similar to that in wild-type neurons (Fig. 6 F). The staining of PKA appeared linear and concentrated in the center of the dendrites in the control neurons at higher magnification (Fig. 6 B). In contrast, the staining of PKA in *map2* $^{-/-}$ appeared punctate, and thus did not appear to be associated with cytoskeletal elements. Since PKA is known to bind to MAP2, it was assumed that PKA was colocalized with MTs in the dendrites. To know whether PKA was associated with cytoskeletal compartments, we treated the cultured neurons with 0.1% Triton X-100. In the control neurons, the amount and the distribution of PKA were similar to the staining without detergent extraction (Fig. 6 C). However, the punctate PKA staining in the dendrites and the staining in the soma were greatly reduced in *map2* $^{-/-}$ neurons (Fig. 6 C′), suggesting the remaining PKA molecules in the somatodendritic compartments in *map2* $^{-/-}$ neurons were not associated with cytoskeletal compartments. We also observed hippocampal and cortical neurons well separated from the neighboring neurons to examine the amount of PKA in the axonal or dendritic compartments. The staining in *map2* $^{-/-}$ dendrites was clearly reduced, but axonal staining was relatively unchanged (unpublished data). In addition, to know the localization and the amount of PKA more precisely at the subcellular level, immunoelectron microscopy was performed in cultured hippocampal neurons. When wild-type neurons were stained with anti-RII β monoclonal antibody and the secondary antibody conjugated with gold particles, followed by silver enhancement, many electron-dense particles were associated with MTs in the dendrite. However, in *map2* $^{-/-}$ neurons, the number of signals reduced significantly. When we quantitated these signals, the density of signals in *map2*

Published August 5, 2002

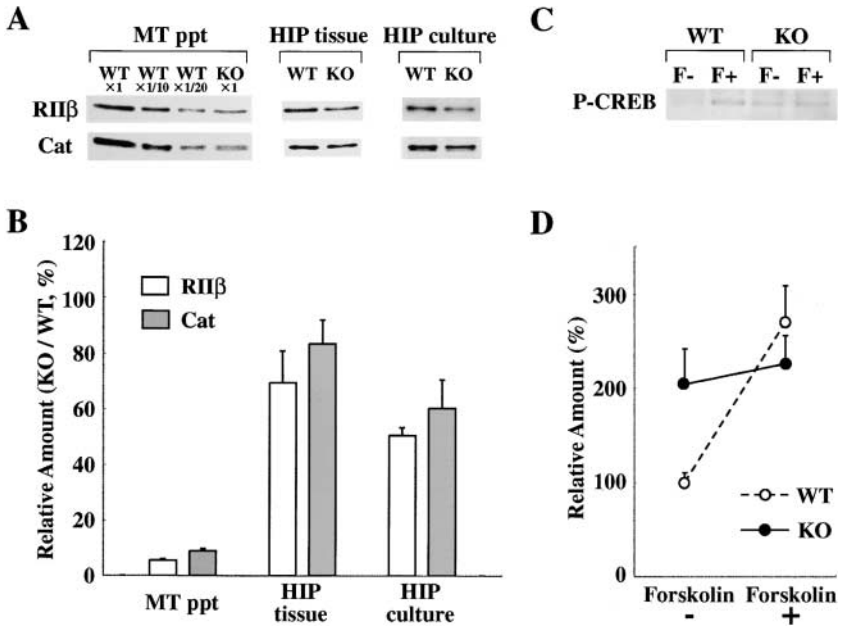

Figure 7. **Reduced amount of PKA and reduced activation (phosphorylation) of CREB after forskolin induction in *map2* $^{-/-}$ mice.** (A) Western blots of the microtubule pellet fraction (MT ppt), the crude extracts from the hippocampal tissue (HIP tissue), and the crude extracts from the cultured neurons (HIP culture) probed with anti–RII β monoclonal antibody (RIIβ) and anti–catalytic subunit antisera (Cat). (B) Quantitation of PKA (RIIβ and Cat) in MT ppt ($n = 3$; one sample was taken from one animal), HIP tissue ($n = 3$), and HIP culture ($n = 3$). The relative amounts of *map2* $^{-/-}$ against wild-type samples are shown. (C) Western blots of phosphorylated CREB. Wild-type (WT) and *map2* $^{-/-}$ (KO) neurons were homogenized before (F−) and 30 min after forskolin stimulation (F+), and equal amounts of samples from wild-type and knockout mice were loaded and separated with polyacrylamide gel. (D) Quantitation of the results of immunoblot in C. The amount of phosphorylated CREB is increased about threefold in wild-type neurons (WT), whereas the amount is nearly unchanged in *map2* $^{-/-}$ neurons (KO). The number of samples and animals are the same as in B.

$^{-/-}$ neurons with PKA antibody was almost equal to that with nonimmune IgG (unpublished data). Even after permeabilization, the PKA molecules were still associated with MTs in wild-type neurons and the density of signals did not differ significantly from that of nonpermeabilized wild-type samples (unpublished data). From these results, PKA molecules are tightly associated with dendritic MTs through MAP2, and thus a part of previously observed globular structures on MTs in wild-type Purkinje dendrites (Fig. 1 C) were assumed to be PKA associated with MAP2.

Total amount of PKA is also reduced in *map2* $^{-/-}$ hippocampal tissue and cultured neurons, and the rate of increase in phosphorylated CREB is less than wild-type neurons after forskolin stimulation

As the amount of PKA was decreased in the somatodendritic compartments of *map2* $^{-/-}$ neurons in vitro and in vivo from the observation of immunofluorescence microscopy and immunoEM, we performed quantitative immunoblot of various fractions with antibodies that recognized RII β and the catalytic subunits of PKA (Fig. 7, A and B). Quite surprisingly, the contents of PKA were greatly reduced in the MT pellet fraction (RII β, ∼5%; catalytic subunit, ∼7% of wild type). Similar reduction was observed when the activity of PKA was quantitated (unpublished data). In addition, PKA was also reduced in the crude homogenate of hippocampal tissues (RII β, ∼70%; catalytic, ∼80% of wild type). When we used the crude extracts from the cultured hippocampal neurons, the PKA content was much more reduced (RII β, ∼50%; catalytic subunit, ∼60% of wild type). These results indicate that the total amount of PKA was reduced in *map2* $^{-/-}$ neurons probably because the PKA molecules anchored and pooled in the MT-rich regions in the dendrites were significantly reduced. To assess possible effects from the reduction of PKA in *map2* $^{-/-}$ neurons, we measured the extent of phosphorylation of a PKA substrate. We quantitated the amount of phosphorylation at Ser133 of CREB, a transcription factor activated by PKA, in cultured hippocampal neurons before and after PKA stimulation by forskolin (Fig. 7, C and D). Before stimulation, the amount of phosphorylated CREB at Ser133 in *map2* $^{-/-}$ neurons was about twofold of that in wild-type neurons. However, the amount of phosphorylated CREB was relatively unchanged (∼1.1-fold increase) even after forskolin stimulation. In contrast, the amount of phosphorylated CREB increased about threefold by stimulation in wild-type neurons. The amount of total CREB did not differ significantly between *map2* $^{-/-}$ and wild-type neurons (unpublished data). From these results, MAP2 is required for controlling the total amount of PKA and proper induction of activated (phosphorylated) CREB.

Discussion

The role of MAP2 in dendrite elongation

MAP2 promotes MT polymerization in vitro. When overexpressed in nonneuronal cells (Lewis et al., 1989; Chen et al., 1992), MAP2 promotes the intracellular MT bundling, and when introduced into Sf 9 insect cells by baculovirus infection, it promotes the formation of MT bundles and the neurite-like process formation (Chen et al., 1992). MAP2 was also considered to be essential in the formation of the dendrites because MAP2 antisense exposure in neuronal cell culture specifically inhibits the elaboration of dendrite-like processes (Caceres et al., 1992).

We observed a reduction in MT density in dendrites of MAP2-deficient mice, which was not described in our previous paper (Teng et al., 2001). Although we did not measure MT density in the dendrites of MAP2 and MAP1B double knockout mice, MAP2 alone is effective in MT polymerization in dendrites from this result. We also observed reduced

Published August 5, 2002

dendritic length in mature MAP2-deficient neurons, but we did not observe a reduction in minor process length in MAP2 single knockout neurons in the previous paper, whereas we observed a reduction in double knockout neurons (Teng et al., 2001). Thus, for initial minor process formation, both MAP2 and MAP1B are required, but for dendritic elongation at later stages, MAP2 alone is important in vitro and in vivo.

The length of dendrites was reduced in MAP2-deficient neurons both in vitro and in vivo, but in vivo only the apical dendrites were shortened and the rate of reduction was smaller (22% in vivo vs. 30% in vitro). The possible explanation for this contradiction is as follows: in vivo, various external factors (growth factors, interaction with other neurons/glias, etc.) may enhance the growth of dendrites and partially compensate for the reduced dendritic extension by the loss of MAP2 in *map2* $^{-/-}$ neurons. However, in dissociated culture where these external factors do not exist, *map2* $^{-/-}$ neurons may show their reduced internal activity in dendritic outgrowth.

Significant reduction of PKA in MT-rich region leads to the reduction in the total amount of PKA in neurons and reduced activation of CREB after forskolin stimulation

We observed a great reduction of PKA in the MT pellet fraction of *map2* $^{-/-}$ neurons (~1/20 [RII β] and 1/15 [catalytic subunit] of wild type) by quantitative immunoblotting. This was confirmed both by measuring activities of PKA in the MT pellet and by immunoelectron microscopy, where the PKA (RII) signals in the MT-rich region of *map2* $^{-/-}$ dendrites were not significantly different from nonimmune controls. As a result of this reduction, the total amounts of PKA in *map2* $^{-/-}$ hippocampal neurons were decreased to about half of those of wild-type neurons. There is a tendency that the amount of the catalytic subunit is less affected than that of RII. This is probably due to the presence of the RI that do not bind to MAP2. Although the amount of RI is much less than RII in neurons and astrocytes, the former is nearly equal to the latter in oligodendrocytes (Stein et al., 1987). This also explains why the reduction rate of PKA in hippocampal tissue is less than that in dissociated hippocampal neurons. In MAP2-deficient neurons, the outer membranous (or submembranous) structures such as the postsynaptic spines and the growth cones, and the internal membranous structures such as the Golgi complex, seem to be the main region of PKA localization from previous papers (De Camilli et al., 1986) and from our immunofluorescence microscopy. In this paper, the localization of PKA seemed to shift from the MT-rich regions to the soluble fraction or these membranous structures. However, considering that the total amount of PKA was still reduced in *map2* $^{-/-}$ neurons, the regions that bound to PKA in *map2* $^{-/-}$ neurons were not sufficient for anchoring all the PKA molecules released from the MT-rich region in the absence of MAP2. This observation strongly indicates that MAP2 is the main PKA-anchoring protein in dendrites. However, in the axonal compartments, the amount of PKA (RII β and the catalytic subunits) did not change significantly as in the dendritic compartments from the observation by immunofluorescence microscopy. This implies that other molecules anchor PKA, especially RII β, in the axons. This may relate to the fact that the affinity of RII β to MAP2 is less than that of RII α. Therefore, RII α seems to be designed to anchor the PKA catalytic subunits to MAP2 in the dendrites, whereas RII β seems to be designed to anchor them to MAP2 in the dendrites and to other anchoring proteins in the axons.

We also observed an increase in the basal phosphorylation of CREB in *map2* $^{-/-}$ neurons compared with wild-type neurons. Phosphorylated CREB only slightly increased after forskolin stimulation in *map2* $^{-/-}$ neurons. Thus, the role of MAP2 seems to trap and store PKA in the dendritic MTs before forskolin stimulation. This role enables PKA to be rapidly released into the cytoplasm to phosphorylate a number of substrates after stimulation.

PKA is also known to phosphorylate a number of substrates including cytoskeletons (Hisanaga et al., 1994) and microtubule-dependent motor proteins (Sato-Yoshitake et al., 1992). A MAP2 knockout mouse can be used for investigating the role of PKA in dendrites by analyzing the phosphorylation of these substrates.

Materials and methods

Hippocampal cell culture

Methods for preparing the hippocampal cell cultures followed those described previously (Harada et al., 1994). Usually, in one set of experiments, fetuses belonging to the same litter were used, the same conditioned medium was used, and feeder glial cells were dissociated from littermate embryos. We also used hippocampal neurons cultured without glial cells for immunofluorescence, immunoelectron microscopy, and for Western blot. The result obtained with either culture protocol was similar therefore, the results were pooled. We followed the neurons photographically and measured the length and counted the number of dendrites as described previously (Harada et al., 1994; Teng et al., 2001). To compare the length of dendrites, we first calculated the average length of dendrites of a neuron by averaging the lengths of all visible dendrites and then obtained the average in each animal by using the average of each neuron.

Immunoblotting

For preparation of crude extracts, the hippocampus was dissected and homogenized with 25 mM Tris, pH 6.8, and 2% SDS, followed by sonication and boiling to lower the viscosity. Cultured cells were lysed in the same buffer and treated in the same manner. Crude extracts were made by centrifuging the homogenates at 20,000 *g* for 15 min at 4°C. Preparation of MT pellet fraction was performed as described previously (Sato-Yoshitake et al., 1989). In brief, the brains were dissected out and homogenized in 3 vol PEM (100 mM PIPES, 1 mM EDTA, and 1 mM $MgCl_2$) including 1 μM PMSF. Crude extracts were prepared by centrifuging the homogenates at 100,000 *g* for 15 min at 4°C. A microtubule polymerizing agent, taxol, was added to the crude extracts to a final concentration of 20 μM. The crude extracts were incubated at 37°C for 15 min, centrifuged at 100,000 *g* for 30 min at 27°C and the resultant pellet was named MT ppt. Protein concentration was determined by BCA protein assay reagent (Pierce Chemical Co.). Equal amounts of crude extracts and MT ppt were loaded and separated with polyacrylamide gel. Proteins were electrophoretically transferred to nylon filters (Millipore). Nylon filters with transferred brain proteins were blocked with 5% skim milk in TBS, incubated in monoclonal antibodies for 1 h, rinsed in TBS and TBS containing 0.05% Tween 20, followed by incubation in rabbit anti–mouse IgG, and incubated for 1 h with ^{125}I-labeled protein A (Amersham Biosciences). Binding was detected by autoradiography using an imaging analyzer (model BAS-2000; Fuji Film). For detection of phospho-CREB, alkaline phosphatase–conjugated secondary antibody was used because the signals obtained by ^{125}I-labeled protein A were not strong enough for quantitation. In this case, quantitation was performed by scanning the Western blot of various amounts of *map2* $^{-/-}$ and control samples. Measurement of the intensity of the bands was performed by NIH

Image software. For the primary antibodies, the following monoclonal antibodies or polyclonal antisera were used: HM-2 (Sigma-Aldrich) for MAP2; 1B6 and 5E6 (Sato-Yoshitake et al., 1989) for MAP1B; 1D1 (Shiomura and Hirokawa, 1987) for MAP1A; tau-1 (Roche) for τ; NN18 (Sigma-Aldrich) for NF-M; DM1A (Sigma-Aldrich) for α-tubulin; anti-PKA RII β monoclonal antibody and anti-PKA catalytic subunit monoclonal antibody (Transduction Laboratory); anti–RII α and RII β polyclonal antisera (gifts from Drs. Walter and Lohmann, University of Würzburg, Würzburg, Germany; De Camilli et al., 1986); anti–PKA catalytic subunit polyclonal antisera (a gift from Drs. Sahara and Fukami, University of Kobe, Kobe, Japan; Sahara et al., 1996); anti–calcium/calmodulin-dependent kinase IIβ monoclonal antibody (Zymed Laboratories); anti–phospho-CREB monoclonal antibody or polyclonal antisera (Cell Signaling Technologies Inc.).

Immunocytochemical analysis

2-, 4-, and 8-wk-old mice were anesthetized with ether and nembutal (WAKO) and perfused with 2% paraformaldehyde in 0.1 M phosphate buffer, pH 7.4. Various parts of brains (cerebellum, cerebral cortex, striatum, hippocampus, and spinal cord) were dissected and stored in the same fixative overnight at RT. The procedure for cryoprotection, freezing, and sectioning was described previously (Harada et al., 1990). Sections were allowed to react with the primary antibodies described previously (Harada et al., 1990) followed by the secondary antibodies (Alexa 488 and 568–conjugated goat anti–mouse or goat anti–rabbit IgG) and Alexa 633-conjugated phalloidin (Molecular Probes). In case of cultured hippocampal neurons, neurons on coverslips were fixed with 2% paraformaldehyde in PBS, pH 6.8, permeabilized in 0.1% Triton in PBS for 5 min at RT, and incubated in the primary and the secondary antibodies as described above. Samples were observed using a laser scanning confocal microscope (model LSM510; ZEISS).

Rapid Golgi staining

Mice were perfused with 2% paraformaldehyde and 2.5% glutaraldehyde in 0.1 M cacodylate buffer, pH 7.4. Hippocampus was dissected and further fixed for 2 h at RT. The dissected hippocampus was washed twice in 3% potassium dichromate in water and incubated in 5% glutaraldehyde and 2.5% potassium dichromate in water at 20°C for 4–5 d. Tissues were washed several times in 0.75% silver nitrate in water and then incubated in 0.75% silver nitrate in water at 20°C for 4–5 d again. 100–150-μm-thick slices were obtained by cutting the tissue perpendicular to the long axis of hippocampus with a microslicer (model DTK-1000; Dosaka EM). The Golgi-stained neurons were observed with a laser scanning confocal microscope by the reflection contrast mode. 10 optical sections (distances between slices were 10 μm) were obtained from one hippocampal slice, and the images were merged to obtain an image as complete as possible of each dendritic tree. To calculate the length of dendrites, we selected three dendrites from one section that appeared to fully extend from the cell body to the tip of the dendrite and use the longest dendrite to represent the section. We took an average of the length of representatives within each genotype (wild type or knockout).

Conventional electron microscopy

Mice were perfused with 2% paraformaldehyde and 2.5% glutaraldehyde in 0.1 M cacodylate buffer, pH 7.4. Tissues (hippocampus, cerebellum, and olfactory bulb) were dissected and further fixed for 2 h at RT. Sections were processed as described previously (Harada et al., 1990) and viewed under an electron microscope (model 2000EX; JEOL) at 100 kV. For analysis of dendritic MT content, blocks of cerebellar samples were sagittally sectioned, and the areas where Purkinje dendrites of large diameter extended perpendicular to the Purkinje cell layer were selected. The blocks were rotated 90° so that these dendrites were cross sectioned. We carefully selected the areas so that the proximal one third of the Purkinje dendrites was sectioned. The Purkinje dendrites with well preserved MTs and internal sER structures were selected from *map2* $^{-/-}$ and wild-type littermates. The areas were photographed at a magnification of 15,000, and the numbers of MTs in the cross sections were counted using a blind-test protocol

Quick-freeze, deep-etch electron microscopy

Cerebellar tissues were dissected, and thin sagittal slices of tissue were saponin-treated and processed for quick-freeze, deep-etch electron microscopy as described previously (Hirokawa et al., 1988). For quantification of cross-bridges, two knockout and two wild-type mice were used. Since the length and diameter of cross-bridges between MTs were similar within each genotype, the values were pooled.

We would like to thank Dr. R. Sato-Harada (University of Gunma) for her generous cooperation throughout this work. We would also like to thank Dr. F. Oyama (University of Tokyo) for his valuable advice on molecular biology, Dr. T. Noda (Cancer Institute) for his advice and generous gifts of various plasmids, Drs. S. Hisanaga (Tokyo Metropolitan University) and M. Inagaki (Aichi Cancer Center Research Institute) for their advice on the measurement of PKA phosphorylation. We would also like to thank Drs. U. Walter, S.M. Lohmann, Y. Ihara (University of Tokyo), S. Sahara, and Y. Fukami for their generous gifts of antibodies, and T. Horie, M. Takano, H. Fukuda, H. Sato, C. Zhao, N. Honma, and many members of Hirokawa's lab for help and discussions.

This work was supported by a Special Grant-in-Aid for Center of Excellence from the Japan Ministry of Education, Science and Culture to N. Hirokawa.

Submitted: 26 October 2001
Revised: 14 June 2002
Accepted: 18 June 2002

References

Abel, T., P.V. Nguyen, M. Barad, T.A.S. Deuel, E.R. Kandel, and R. Bourtchouladze. 1997. Genetic demonstration of a role for PKA in the late phase of LTP and in hippocampus-based long-term memory. *Cell.* 88:615–626.

Caceres, A., J. Mautino, and K.S. Kosik. 1992. Suppression of MAP2 in cultured cerebellar macroneurons inhibits minor neurite formation. *Neuron.* 9:607–618.

Chen, J., Y. Kanai, N.J. Cowan, and N. Hirokawa. 1992. Projection domains of MAP2 and tau determine spacing between microtubules in dendrites and axons. *Nature.* 360:674–677.

De Camilli, P., M. Moretti, S.D. Donini, U. Walter, and S.M. Lohmann. 1986. Heterogeneous distribution of the cAMP receptor protein RII in the nervous system: evidence for its intracellular accumulation on microtubules, microtubule-organizing centers, and in the area of the Golgi complex. *J. Cell Biol.* 103:189–203.

Dinsmore, J.H., and F. Solomon. 1991. Inhibition of MAP2 expression affects both morphological and cell division phenotypes of neuronal differentiation. *Cell.* 64:817–826.

Goedert, M., R.A. Crowther, and C.C. Garner. 1991. Molecular characterization of microtubule-associated proteins tau and MAP2. *Trends Neurosci.* 14:193–199.

Glantz, S.B., J.A Amat, and C.S. Rubin. 1992. cAMP signaling in neurons: patterns of neuronal expression and intracellular localization for a novel protein, AKAP 150, that anchors the regulatory subunit of cAMP-dependent protein kinase II beta. *Mol. Biol. Cell.* 3:1215–1228.

Harada, A., K. Sobue, and N. Hirokawa. 1990. Developmental changes of synapsin I subcellular localization in rat cerebellar neurons. *Cell Struct. Funct.* 15:329–342.

Harada, A., K. Oguchi, S. Okabe, J. Kuno, S. Terada, T. Ohshima, R. Sato-Yoshitake, Y. Takei, T. Noda, and N. Hirokawa. 1994. Altered microtubule organization in small-calibre axons of mice lacking tau protein. *Nature.* 369: 488–491.

Harada, A., Y. Takei, Y. Kanai, Y. Tanaka, S. Nonaka, and N. Hirokawa. 1998. Golgi vesiculation and lysosome dispersion in cells lacking cytoplasmic dynein. *J. Cell Biol.* 141:51–59.

Hirokawa, N., S. Hisanaga, and Y. Shiomura. 1988. MAP2 is a component of crossbridges between microtubules and neurofilaments in the neuronal cytoskeleton: quick-freeze, deep-etch immunoelectron microscopy and reconstitution studies. *J. Neurosci.* 8:2769–2779.

Hirokawa, N. 1994. Microtubule organization and dynamics dependent on microtubule-associated proteins. *Curr. Opin. Cell Biol.* 6:74–82.

Hisanaga, S., Y. Matsuoka, K. Nishizawa, T. Saito, M. Inagaki, and N. Hirokawa. 1994. Phosphorylation of native and reassembled neurofilaments composed of NF-L, NF-M, and NF-H by the catalytic subunit of cAMP-dependent protein kinase. *Mol. Biol. Cell.* 5:161–172.

Kalcheva, N., J. Albala, K. O'Guin, H. Rubino, C. Garner, and B. Shafit-Zagardo. 1995. Genomic structure of human microtubule-associated protein 2 (MAP-2) and characterization of additional MAP-2 isoforms. *Proc. Natl. Acad. Sci. USA.* 92:10894–10898.

Lewis, S.A., I.E. Ivanov, G.H. Lee, and N.J. Cowan. 1989. Organization of microtubules in dendrites and axons is determined by a short hydrophobic zipper in microtubule-associated proteins MAP2 and tau. *Nature.* 342:498–505.

Malleret, G., U. Haditsch, D. Genoux, M.W. Jones, T.V.P. Bliss, A.M. Vanhoose, C. Weitlauf, E.R. Kandel, D.G. Winder, and I.M. Mansuy. 2001. Inducible

and reversible enhancement of learning, memory, and long-term potentiation by genetic inhibition of calcineurin. *Cell.* 104:675–686.

Matus, A. 1994. Stiff microtubules and neuronal morphology. *Trends Neurosci.* 17: 19–22.

Sahara, S., K. Sato, H. Kaise, K. Mori, A. Sato, M. Aoto, A.A. Tokmakov, and Y. Fukami. 1996. Biochemical evidence for the interaction of regulatory subunit of cAMP-dependent protein kinase with IDA (Inter-DFG-APE) region of catalytic subunit. *FEBS Lett.* 384:138–142.

Sato-Yoshitake, R., Y. Shiomura, H. Miyasaka, and N. Hirokawa. 1989. Microtubule-associated protein 1B: molecular structure, localization, and phosphorylation-dependent expression in developing neurons. *Neuron.* 3:229–238.

Sato-Yoshitake, R., H. Yorifuji, M. Inagaki, and N. Hirokawa. 1992. The phosphorylation of kinesin regulates its binding to synaptic vesicles. *J. Biol. Chem.* 267:23930–23936.

Shiomura, Y., and N. Hirokawa. 1987. Colocalization of microtubule-associated protein 1A and microtubule-associated protein 2 on neuronal microtubules in situ revealed with double label immunoelectron microscopy. *J. Cell Biol.* 104:1575–1578.

Stein, J.C., M. Farooq, W.T. Norton, and C.S. Rubin. 1987. Differential expression of isoforms of the regulatory subunit of type II cAMP-dependent protein kinase in rat neurons, astrocytes, and oligodendrocytes. *J. Biol. Chem.* 262:3002–3006.

Takemura, R., S. Okabe, T. Umeyama, Y. Kanai, N.J. Cowan, and N. Hirokawa. 1992. Increased microtubule stability and alpha tubulin acetylation in cells transfected with microtubule-associated proteins MAP1B, MAP2 or tau. *J. Cell Sci.* 103:953–964.

Teng, J., Y. Takei, A. Harada, T. Nakata, J. Chen, and N. Hirokawa. 2001. Synergistic effects of MAP2 and MAP1B knockout in neuronal migration, dendritic outgrowth, and microtubule organization. *J. Cell Biol.* 155:65–76.

Theurkauf, W.E., and R.B. Vallee. 1982. Molecular characterization of the cAMP-dependent protein kinase bound to microtubule-associated protein 2. *J. Biol. Chem.* 257:3284–3290.

Vallee, R.B., M.J. DiBartolomeis, and W.E. Theurkauf. 1981. A protein kinase bound to the projection portion of MAP 2 (microtubule-associated protein 2). *J. Cell Biol.* 90:568–576.

Ventra, C., A. Porcellini, A. Feliciello, A. Gallo, M. Paolillo, E. Mele, V.E. Avvedimento, and G. Schettini. 1996. The differential response of protein kinase A to cyclic AMP in discrete brain areas correlates with the abundance of regulatory subunit II. *J. Neurochem.* 66:1752–1761.